Advances in Engineering Software 99 (2016) 27–35

Contents lists available at ScienceDirect

Advances in Engineering Software

journal homepage: www.elsevier.com/locate/advengsoft

Optimization of foam-filled double ellipse tubes under multiple loading cases

Qiang Gao[a], Liangmo Wang[a,*], Yuanlong Wang[a], Fuxiang Guo[b], Zunzhi Zhang[b]

[a] School of Mechanical Engineering, Nanjing University of Science and Technology, Nanjing, P.R. China
[b] Nanjing Iveco Automobile Co. Ltd., Nanjing 210028, China

ARTICLE INFO

Article history:
Received 26 February 2016
Revised 7 April 2016
Accepted 1 May 2016

Keywords:
Foam-filled double ellipse tube
Crashwothiness
Multiobjective optimization
Multiple loading

ABSTRACT

In this paper, a novel foam-filled double ellipse tube (F-DET) is proposed. First, the circle and ellipse tubes with three different configurations(hollow, foam-filled, double foam-filled) are investigated under axial and oblique impact by using the nonlinear finite element code LS-DYNA. The numerical results showed that the F-DET tube has the best crashworthiness performance than tubes with other configurations. Then to optimize the F-DET tube, the Kriging model about the radial rate f, thickness of wall t and foam density ρ_f is constructed. Based on the Kriging model, the multiobjective particle swarm optimization (MOPSO) algorithm is utilized to achieve the optimized F-DET tube, foam-filled ellipse(F-ET) tube and foam-filled double circle(F-DCT) tube on the maximizing specific energy absorption (SEA) and minimizing peak crush force (PCF) under multiple loading angles. It can be found that the F-DET tube has better crashworthiness performance than F-ET tube and F-DCT tube. This indicates F-DET tube can be a potential energy absorber under the multiple loading cases.

1. Introduction

By development of technology, the number of vehicles and their speed have increased and the possibility of car crashes and human injuries has increased as a result. Therefore, the researchers focus more attention to the crashworthiness of the vehicle safety. At the same time, the fuel consumption is another aspect on the designing of the vehicle which could not be ignored. Thus, to improve the energy absorption of a material, the thin walled structures have been applied in many cases, especially thin walled tubes. Superior energy absorption capability of thin-walled tubes lays in the progressive and controllable plastic deformation modes. Extensive research efforts were conducted to investigate the crushing behavior of thin-walled tubes under quasi-static and dynamic loading [1].

To enhance energy absorption without much increase in mass, cellular materials or structures including metallic foams [2–8], synthetic foams [9–12], natural cellular materials [13] and honeycombs [14] are used to fill the tubes. Some other research focus on the multi-tube usage [14–18] and generating corrugated/grooved surfaces on the tubes. To predict the crashworthiness of the thin walled tubes, Hanssen et al. [19,20] presented the close-form formulas to predict the behaviors of foam-filled aluminum tubes under both quasi-static and dynamic loading conditions. They showed that the total energy absorption of a foam-filled tube exceeded the sum of individual energies absorbed in empty column and form filler due to the interaction between foam and column wall. Recently, considering the crashing performance of the vehicle in real world, the deformation mode of the tubes under the oblique loading has been analyzed and some novel structures are proposed. The crush behavior of mild steel square columns was analyzed by Han and Park [21], indicating that from the axial to the bending collapse mode, there was a critical load angle at the transition place. Li et al. [22] paid attention to the aluminum foam circular tubes and did some experiments. As for the tapered tubes, the tapered rectangle tubes had more advantages than straight tubes under an oblique impact has been concluded by Nagel and Thambiratnam [23–25]. To make more effective use of various foam-filled thin-wall structure systems, some researchers [26,27] attempted to simultaneously optimize foam density and wall thickness to seek best possible combination for enhancing crashworthiness.

Meanwhile, the double tubes gains increasing attention from the researchers due to the advantages on the crashworthiness under both axial and oblique impact. Goel [3] compared the energy absorption of empty and Al foam filled bi-tubular and tri-tubular configurations to empty and foam-filled single circular and square tubes numerically. The results revealed that energy absorption capacity of Al foam-filled bi-and tri-tubular structures were higher in contrast to single foam-filled tubes. Guo et al. [28] investigated the crashworthiness of double circular tubes under bending

* Corresponding author. Fax: +8684315425.
E-mail address: liangmowang_njust@163.com (L. Wang).

http://dx.doi.org/10.1016/j.advengsoft.2016.05.001
0965-9978/

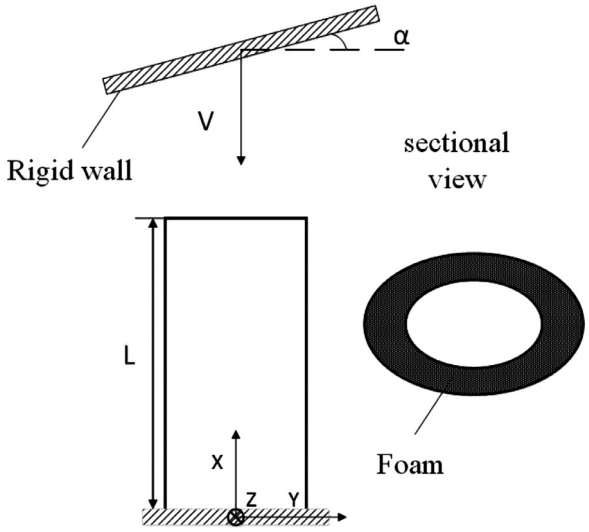

Fig. 1. Schematic diagram of tube under oblique impact.

conditions using experimental and numerical testing, which indicates the superiority of the ability absorbing the energy. Experimental and finite element analyses were performed on bitubular square thin-walled tubes with different arrangements under quasi-static axial compression loading by Kashani [29], and the effect of length difference in inner and outer tubes was studied.

In this paper, a novel foam-filled double ellipse tube is proposed. First, the hollow tubes (H-T), foam-filled tube (F-T), foam-filled double tube (F-DT) with two different cross-sections (circle, ellipse) are analyzed using the nonlinear explicit FEA code LS-DYNA about the crushing behavior. The specific energy absorption (SEA, absorbed energy per unit mass) and peak crushing force (PCF) under axial and oblique impact are compared. It will show that the foam-filled double ellipse tube (F-DET) has the best crashing performance under axial and minor oblique impact. To achieve the optimal F-DET tube, some geometry parameters are chosen to design the DOE experiments. Based on this, a Kriging approximation model is established to formulate the objective and constraint functions. Then the multiobjective particle swarm optimization (MOPSO) algorithm is used as the optimizer for solving the multiobjective optimization design (MOD) problems. Finally, the crashing performances of the optimal F-DET tube, the foam-filled ellipse tube(F-ET) and the foam-filled double circle(F-DCT) tube are compared to reveal the advantage of the F-DET tube.

2. Materials and methods

2.1. Description of geometrical features

To simplify the vehicle collision model, the thin walled tube (Fig. 1) is fixed on the bottom end and the rigid wall is given an initial velocity (v = 10 m/s). The structure considered in this study is F-DET tube with the length L=250 mm, wall thickness t=2.0 mm and foam density ρf=0.206 g/cm^3. The inner tube and the outer tube share the same center. The normal of the rigid wall is in the X–Z plane and has an oblique angle α with the axis of the tube. The geometrical parameter of the cross-section can be get from the Fig. 2. And the radial rate f is defined as follows:

$$f = b/a \tag{1}$$

2.2. Material properties

Both the outer and inner tube wall is made of aluminum alloy with densityρ=2700 kg /m^3, Young's modulus E=68 GPa, and

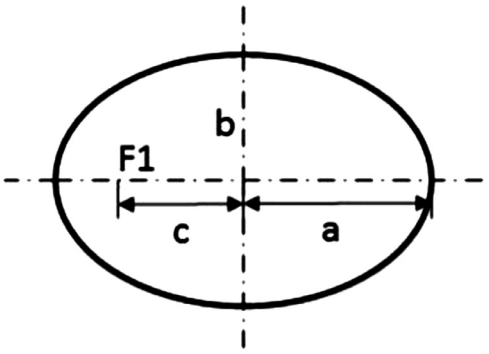

Fig. 2. Schematic diagram of ellipse tub parameter.

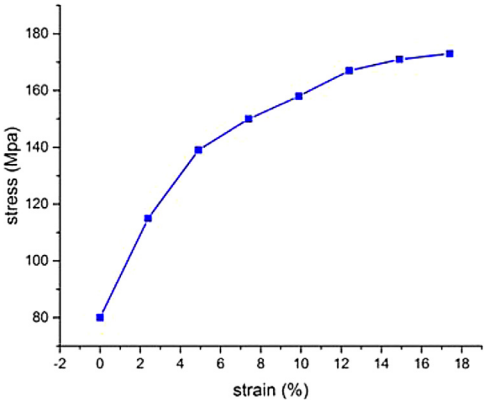

Fig. 3. Tensile stress–strain curve of AA6060.

Poisson's ratio υ=0.3. Fig. 3 indicates the stress-strain curve of the tube material via uniaxial test. The constitutive law is based on an elastoplastic material model with von Mises's isotropic plasticity algorithm and plastic hardening [30]. Since the aluminum is insensitive to the strain rate, this strain-rate effect is neglected in the FE model [31].The constitutive behavior of the aluminum column was modeled via the piece wise linear plasticity material model, Mat 24, in LS-DYNA.

The foam material is based on an isotropic uniform material model developed by Deshpande and Fleck [32]. The yield criterion of such a material is defined as follows:

$$\varphi = \hat{\sigma} - Y \le 0 \tag{2}$$

where Y is the yield stress, and the equivalent stress $\hat{\sigma}$ is given as

$$\hat{\sigma}^2 = \frac{\sigma_e^2 + \alpha^2\sigma_m^2}{1 + (\alpha/3)^2} \tag{3}$$

where σ_e represents the von Mises effective stress and σ_m is the mean stress. For the aluminum foam, α=2.12 is used.

The strain hardening rule is implemented in the material model as follows:

$$Y = \sigma_p + \gamma\frac{\hat{\varepsilon}}{\varepsilon_D} + \alpha^2 \mathrm{in}\left(\frac{1}{1-(\hat{\varepsilon}/\varepsilon_D)^\beta}\right) \tag{4}$$

where $\hat{\varepsilon}$ is an equivalent strain. $\sigma_p, \alpha_2, \gamma, \frac{1}{\beta}, E_p$, and ε_D are the material parameters which are related to the foam density as [33]

$$\left(\sigma_p, \alpha_2, \gamma, \frac{1}{\beta}, E_p\right) = C_0 + C_1\left(\frac{\rho_f}{\rho_{f0}}\right)^\kappa$$

$$\varepsilon_D = -\ln\left(\frac{\rho_f}{\rho_{f0}}\right) \tag{5}$$

in which ρ_f is the foam density, ρ_{f^0} the density of the base material, and C_0, C_1 and κ are the constants as listed in Table 1. In

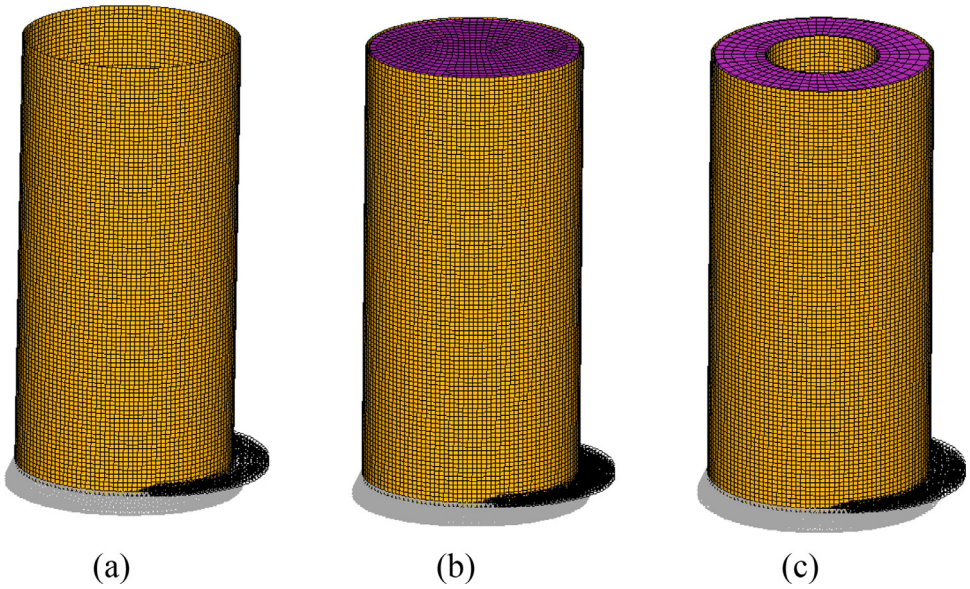

Fig. 4. The finite element model of cylindrical tubes. (a) H-ET, (b) F-ET and (c) F-DET.

general, the constants are different with different directions or manufacture technologies. But this difference is not on our focus in the current study, and it is assumed that the foam used here is in the same direction with the same manufacture process similarly to literature [33].

2.3. Finite element models of the structures

In this paper, the tubes wall were modeled using four node shell continuum elements with five integration points along the element's thickness direction. Moreover, the foam filled tube was modeled using eight node continuum elements with a reduced integration technique combined with the hourglass control. After the mesh convergence test, the shell elements with 2.5 mm × 2.5 mm for the tube and the solid elements 4 mm × 4 mm × 4 mm for the foam are finally adopted to simulate the crushing process of foam-filled tubes. Fig. 4 shows the FE model of the hollow ellipse tube(H-ET), foam-filled ellipse tube(F-ET), and foam-filled double ellipse tube(F-DET). Take the F-DET tube as example, there are 18,600 2d elements and 17,360 3d elements in the FE model. An automatic surface to surface contact algorithm is defined between the aluminum foam elements and outer and inner tube shell elements. To take into account the contact between the tube walls during deformation and avoid interpenetration of folding mode, an automatic single surface contact algorithm is used to the walls of outer and inner tubes. Lastly, the node to surface contact is modeled between the rigid wall and the thin-walled tube. For all the contacts, the static and dynamic coefficients of friction are set as 0.3 and 0.2, respectively.

3. Results and discussion

3.1. Model validation

First, the FE result of the hollow circle tube(H-CT) under axial loading condition is validated by comparing with a close-form formula of the mean crushing force (MCF), proposed by Wierzbicki et al. [33],as

$$MCF = 13.06\sigma_0 {b_m}^{1/3} t^{5/3} \quad (6)$$

Where σ_0 is the energy equivalent flow stress of tube material, b_m and t are width and wall thickness of tube, respectively. Li

Table 1
Stress strain corresponding relationship for arbitrary foam density.

	σ_p (Mpa)	α_2 (Mpa)	$\frac{1}{\beta}$	γ (Mpa)	E_p (Mpa)
C_0 (Mpa)	0	0	0.22	0	0
C_1 (Mpa)	720	140	320	42	3.3e5
κ	2.33	0.45	4.66	1.42	2.45

Fig. 5. Comparison of experiment and simulation model.

[34] compared the MCF between the FE and close-form solutions by testing the H-CT tubes with three different wall thickness and reveal that there is a good agreement between these two solutions. Fig. 5 exhibits the comparison, which demonstrates that the FE simulation agrees fairly well with the experimental results in terms of deformation pattern [34].

Second, the validation of the accuracy of the foam-filled circle tube has been carried out by Li et al. [35]. The model established by [35] was under a quasi-static oblique loading with a constant loading speed of 0.09 mm/s. The material of the tube was aluminum alloy AA6063 T6. The geometric of the tube were length 90 mm, and outer and inner diameters of 38 mm and 24 mm, respectively. The thicknesses of the tube wall tube i.e., the inner and the outer, were 2.0 mm and 1.2 mm, respectively. Table 2 compares the FE results of the model and experiment results in [35] under different angles of impact for foam-filled double circle tube. The error between the FE simulation and experiments is less than the

Table 2
Difference between FE and experimental tests.

	Impact angle (°)	FE	Experiment (Li)	Error(%)
Energy absorption (J)	0	3247.24	3524	2.74
Specific energy absorption (J/g)		25.93	26.7	2.88
Energy absorption (J)	15	3197.28	3286	2.69
Specific energy absorption (J/g)		24.25	24.8	2.19

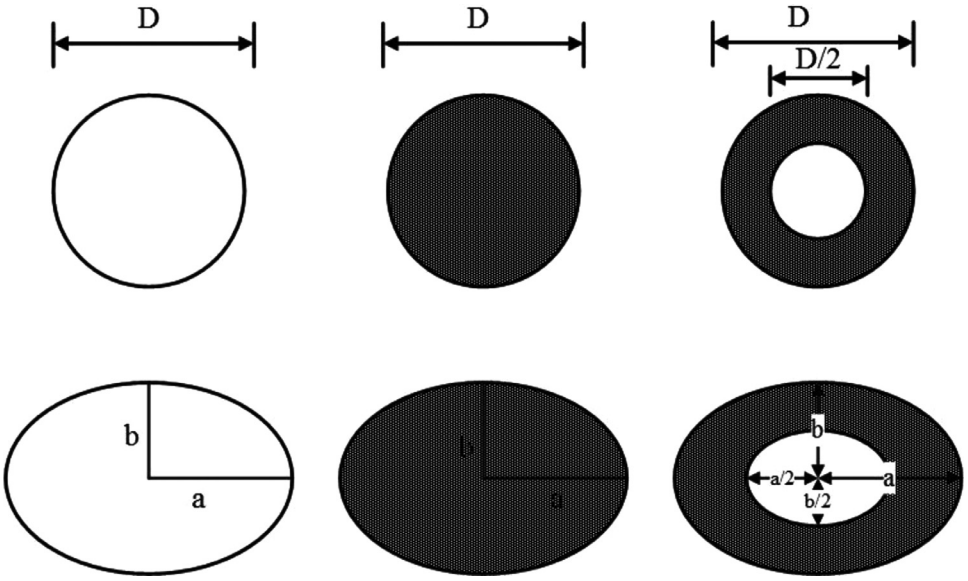

Fig. 6. Schematic of tubes with different cross-section shapes.

3%. As a result, the FE model in this paper is convincing. And it is reasonable to extend the model to the F-DET tubes.

3.2. Structural crashworthiness indices

To evaluate the crashworthiness performance properly, it is essential to define the crash criteria. Energy absorption (EA), specific energy absorption (SEA), mean crushing force (MCF) and peak crushing force (PCF), and have been widely used to estimate the energy absorption capabilities of energy absorbers. The EA for a given structural deformation is defined as:

$$EA = \int_0^d F(x)dx \tag{7}$$

where d is the effective stroke length [33], which is taken as 0.7 L in the current study, and L is the total length of the energy absorbing structure.

The SEA is defined as the ratio of the absorbed energy to the mass of the structure, m, as follows:

$$SEA = \frac{E}{M} \tag{8}$$

The *MCF* for a given structural deformation is defined as:

$$MCF = \frac{EA}{d} \tag{9}$$

The PCF means peak crushing force during the whole impact process and is defined as:

$$PCF = \max[F(l)] \tag{10}$$

Where $F(l)$ is the force when the stroke length equal l.

In this study, in order to bring the load angle uncertainty effect into structural SEA calculation under oblique loading, a new crashworthiness index, SEA_α, is proposed and defined as follows:

$$SEA_\alpha = \sum_{i=0}^{n} SEA^{\alpha i} w^{\alpha i} \tag{11}$$

where the symbol α implies that SEA_α is a composite index involving the structural *SEA* under multiple oblique loadings; $SEA^{\alpha i}$ denotes the structural SEA under the ith oblique load with angle α_i and $w^{\alpha i}$ is the corresponding weighting factor to this $SEA^{\alpha i}$.

3.3. Crashworthiness comparison of tubes with different configurations

Numerical analyses are carried out using the validated FE models to compare the crushing behaviors of these six different tube configurations (i.e. H-CT, H-ET, F-CT, F-ET, F-DCT and F-DET tubes). Fig. 6 shows the cross sections of the tubes with the same material AA6063-T6 and length (L = 250 mm). These tubes are loaded by a rigid wall with a loading angle α varying from 0° to 30° with an interval of 5°. The rigid wall impacted the top of the tubes at an initial velocity of v = 10 m/s until crash distance equals 70% of the total length.

Fig. 7 depicts the deformation mode of F-DET tubes under multiple loading. It is obvious that the deformation mode changed with the increase of the impact angle, which have vital effect on the absorbing energy of the tubes. Fig. 8 denotes the SEA of the tubes with different configurations. It is obvious that SEA of the tubes decrease with the increment of the impact angle. This is due to the change of the deformation pattern. Progressive axial collapse dominates when the impact angle is minor and global bending will dominate with the increment of the impact angle. The energy absorbed by progressive axial collapse is larger than that by global bending has been revealed by many researchers. And there is always a critical impact angle at which the deformation mode of the

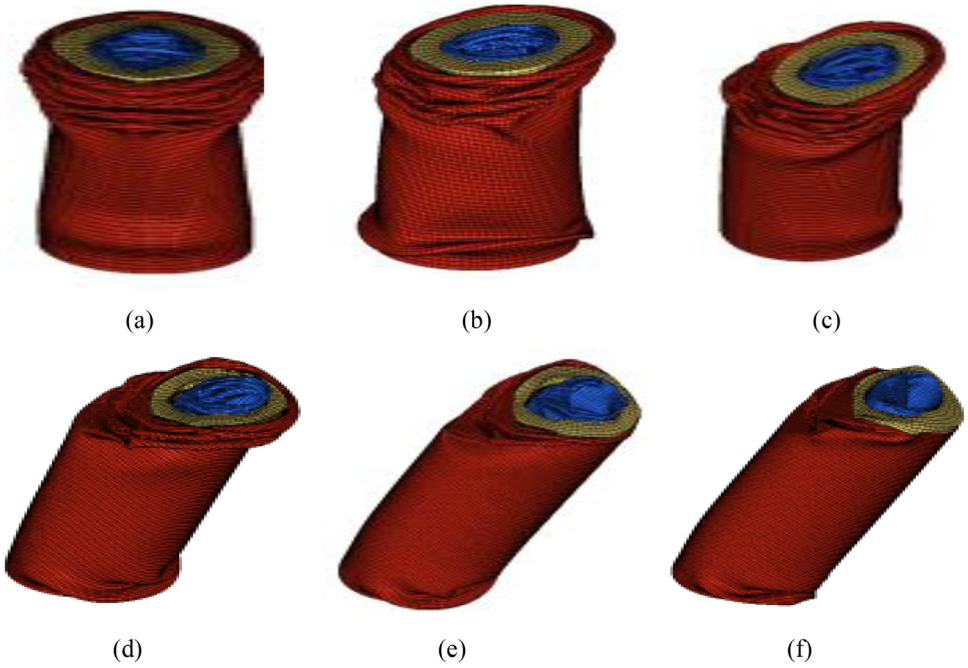

Fig. 7. Deformation modes of the single-cell ellipse tube under different load angles (a) 0° (b) 5° (c) 10° (d)15° (e) 20° (f) 30°.

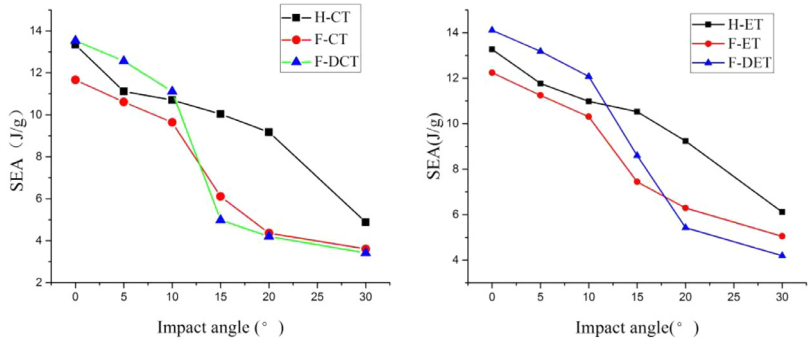

Fig. 8. SEA of the tubes with different configurations (a) Circle tubes (b) Ellipse tubes.

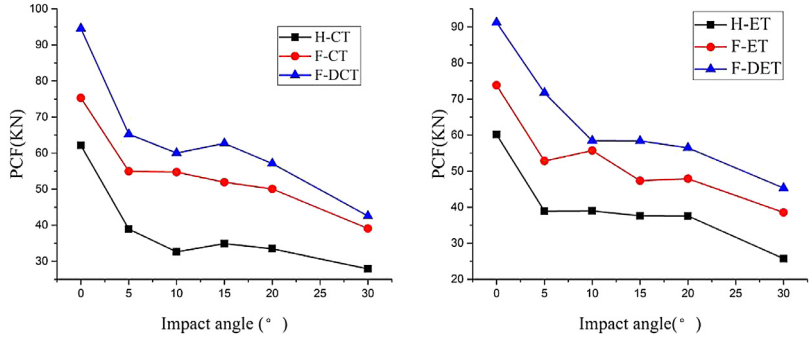

Fig. 9. PCF of the tubes with different configurations (a) Circle tubes (b) Ellipse tubes.

tubes changed. It can be concluded from Fig. 8(a) that the critical angle of the circle tubes is between the 10° and 15°. The F-DCT tube has the best crashworthiness performance when the impact angle is lower than 10°. However, under the lager impact angle, the SEA of the H-CT tube is highest. It can be supposed that the foam has bad performance on bear the oblique impacting. Under the pure axial and minor oblique impact, the foam can enhance the ability of absorbing the energy. In Fig. 8(b), the SEA of the F-DET tube decrease more softly comparing the F-DCT tube when the impact angle equals 15°. This indicates that the ellipse tube has superiority on the bearing oblique impact, especially the F-DET tube.

Fig. 9 summarize the PCF of the tubes with different configurations under different impact conditions. It is evident that the PCF decreases with the increasing of load angle for each tube, which means the maximum PCF occurs when the tube is loaded pure axially. In addition, the PCF of the foam-filled double tubes is always higher than the other two kinds of tubes due to the lager weight.

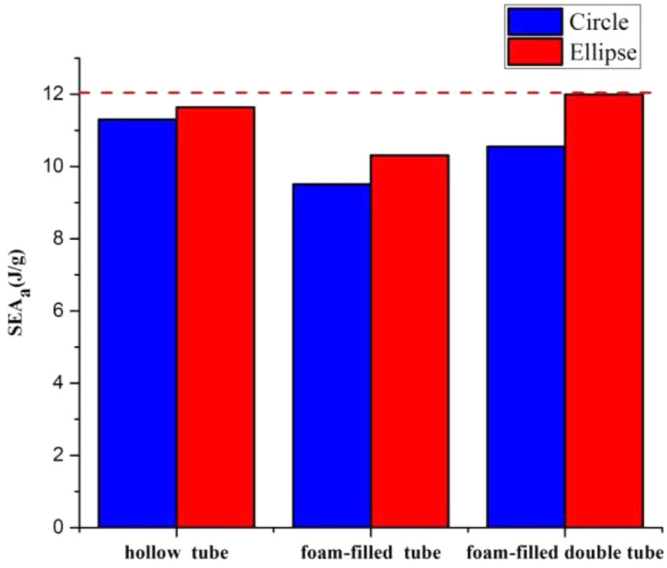

Fig. 10. SEA_α of tubes with different configurations.

Therefore, the merits of the foam-filled double tubes can not be erased according this.

To compare the comprehensive performance of the different tubes under oblique impact, we select load angles $\alpha = 0°$, 5°, 10°, 15° in Eq. (11) to calculate of SEA_α of these tubes. The reason to choose these angles is that in the practical world, the vehicle crash in most axial impact and minor oblique impact. It is rare that the vehicle crash as a lager impact angle. The weighting factors for different load angles should be determined based on the occurrence probabilities of each crash angle in real applications. Here the weighing factors are all set $w^{\alpha i} = 1/4$. It is obvious (Fig. 10) that the foam-filled double ellipse tubes has the best crashworthiness performance. The foam-filled double circle tube performs not well as imagine due to the bad performance when the impact angle equals 15°. Therefore, the F-DET tube is a potential energy absorber under multiple loading.

To further study the effects of foam density, wall thickness on the crashworthiness of foam-filled double ellipse tubes under multiple impact angles. Figs. 11 and 12 depict the effects of the three parameters on the SEA_α and PCF^0. It can be concluded that some effect of the parameters are nonlinear on the SEA_α. Thus, to further improve its crashworthiness, multiobjective optimization design(MOD) is conducted by adopting multiobjective particle swarm optimization (MOPSO) algorithm in the following section.

4. Multiobjective optimization

4.1. Problem description

To improve the crashworthiness of the F-DET tube, there are two indicators needed to be considered. As an energy absorber, the structure is expected to absorb as much impact energy as possible per unit mass. Thus, SEA should be chosen as an objective function and maximized in the crashworthiness optimization problem. To take multiple loading into account, the SEA_α is considered as the indicator instead. In this paper, the impact angle $\alpha = 0°$, 5°, 10°, 15° are chosen to calculate the overall SEA and the weighting factors for each angle is 0.25. However, an overly high PCF often leads to severe injury or even death of occupant. Thus, PCF^0 is set as another objective function and minimize it in the optimization problem. As a result, the multiobjective optimization of the F-DET and F-ET tubes can be formulated as follows:

$$\begin{aligned} &\min \left\{ -SEA_\alpha(f,t,\rho_f), PCF^0(f,t,\rho_f) \right\} \\ &\text{S.t. } 0.5 \le f \le 1 \\ &1\,\text{mm} \le t \le 2.5\,\text{mm} \\ &0.027\,\text{g/cm}^3 \le \rho_f \le 0.327/\text{cm}^3 \end{aligned} \tag{12}$$

4.2. Surrogate model and error metrics

Various surrogate model techniques have been widely used in crashworthiness design. The response surface method (RSM), moving least square method (MLS), Kriging and feed-forward neural networks are some examples. In this regard, the Kriging method has exhibited a fairly good accuracy for highly nonlinear design responses [36] and will be employed to the construct surrogate models for design criteria of SEA_α and PCF^0 in this paper. To reduce the number of required sample points for constructing the Kriging meta-models to formulate the crashworthiness objectives, the D-optimal DOE method was used. Meanwhile, this method helps

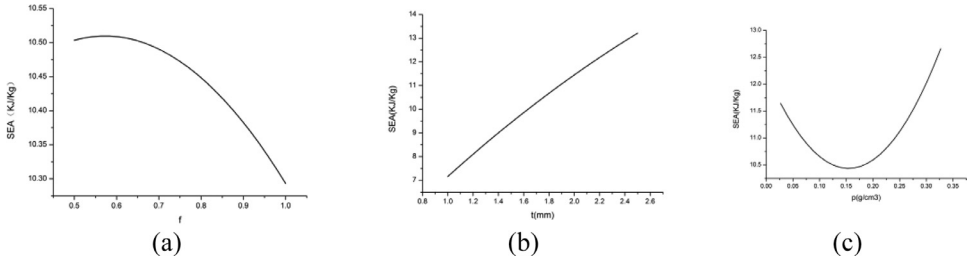

Fig. 11. The effects of the parameters on the SEA_α (a) f (b) t (c) *pf*.

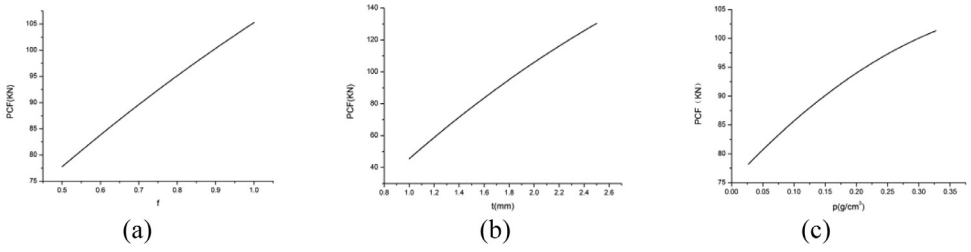

Fig. 12. The effects of the parameters on the PCF^0 (a) f (b) t (c) *pf*.

Table 3
Design matrix of thin-walled structures for crashworthiness.

n	f	t (mm)	ρf (g/cm^3)	F-DET		F-ET	
				SEA^{α} (J/g)	PCF^0(KN)	SEA^{α} (J/g)	PCF^0(KN)
1	0.5	1	0.027	8.375	38.303	6.253	25.162
2	0.5	1.5	0.127	9.623	61.609	7.491	42.315
3	0.5	2	0.227	12.179	95.171	9.920	67.18
4	0.5	2.5	0.327	14.791	133.309	12.486	99.98
5	0.66	1	0.127	7.608	41.251	6.206	28.604
6	0.66	1.5	0.027	10.988	61.548	8.798	41.388
7	0.66	2	0.327	13.501	111.041	12.480	89.144
8	0.66	2.5	0.227	13.488	129.942	11.181	90.044
9	0.83	1	0.227	7.249	50.52	7.041	40.003
10	0.83	1.5	0.327	11.981	90.428	10.628	75.322
11	0.83	2	0.027	12.433	93.031	10.431	61.309
12	0.83	2.5	0.127	12.905	127.555	10.272	84.465
13	1	1	0.327	9.595	67.838	8.508	61.714
14	1	1.5	0.227	9.306	78.257	7.608	58.265
15	1	2	0.127	11.237	127.91	8.736	66.163
16	1	2.5	0.027	14.563	98.731	11.102	82.789

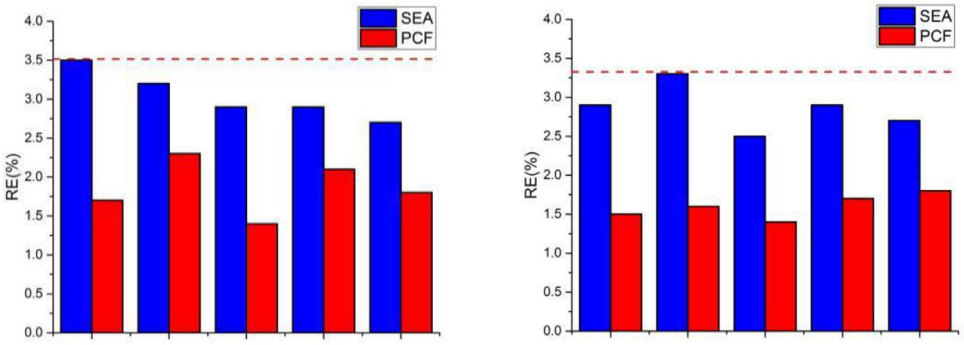

Fig. 13. Relative errors of design objectives of S-TET tube (a) SEA_{α} (b) PCF^0.

to achieve a meta-model with good quality. The DOE experiment results of the F-DET and F-ET tubes are summarized in Table. 3.

The constructed Kriging models need to be validated since qualities of these meta-models affect directly the optimization results. To validate these models at a reasonable cost, five extra random points were generated in the design domains of the two types of columns. To measure the degree of approximation of the Kriging models to the FEA results, the relative error (RE) can be evaluated as:

$$RE = \left| \frac{y(x) - \hat{y}(x)}{y(x)} \right| \tag{13}$$

where $\hat{y}(x)$ is the radial basis functions models and $y(x)$ is the finite element result.

Fig. 13 shows the percentage of relative errors (% RE) of the initial sample points for the FEA and the RBF in five random sample points. The SEA_{α} and PCF^0 show that the RE for these Kriging meta-model approximations was less than 4% and 2.5%, respectively. Thus, it can be assumed that the Kriging model for the objective functions (SEA_{α} and PCF^0) provided sufficient accuracy for design optimization.

4.3. Optimization results

In our study, the multiobjective particle swarm optimization (MOPSO) algorithm (Table 4) is utilized to generate the Pareto front of the two conflicting objectives SEA_{α} and PCF^0. Compared with other multiobjective optimization algorithms, the multiobjective article swarm optimization has the advantages on it is relatively fast convergence and well-distributed Pareto front. The details of MOPSO can be consulted from Ref. [37]. Fig. 14 depicts the Pareto front of the F-DET, F-ET and F-DCT tubes with load angle uncertainty. It can be concluded that there is a conflict relationship between the SEA_{α} and PCF^0 for both the tubes. It is obvious that the crashworthiness performance of the F-DET tube is better than the F-ET and F-DCT tubes. If the PCF of the structure is needed to be constrained under the level of 80 k N when it is used as an energy absorber in engineering, the optimal design corresponds to the Pareto point marked as solid triangles in Fig. 14, and its detailed design parameters are listed in Table 5. Meanwhile, we established the FE model for the optimal design of F-DET, F-ET and F-DCT tubes. The comparison between the FEA results and the approximation results are shown in Table 5. It can be found that the errors are less than 4%. The error of SEA_{α} is bigger than that of

Table 4
The parameter setting of MOPSO algorithm.

MOPSO parameter name	Value
Population size	100
External archive size	100
Inertial weight	0.73
Personal learning coefficient	1.50
Global learning coefficient	1.50

Table 5
Optimal design parameters of tubes for PCF constrained under 80 KN.

Tubes	f	t (mm)	ρf (g/cm^3)	SEA^{α}(J/g)			PCF^0(KN)		
				Kriging	FEA	Error(%)	Kriging	FEA	Error(%)
F-DET	0.564	1.771	0.035	12.586	13.021	3.46	80.570	79.589	1.21
F-ET	0.648	1.785	0.312	11.621	11.996	3.22	79.140	78.252	1.01
F-DCT	1	1.985	0.057	11.582	11.783	2.01	79.932	79.012	1.15

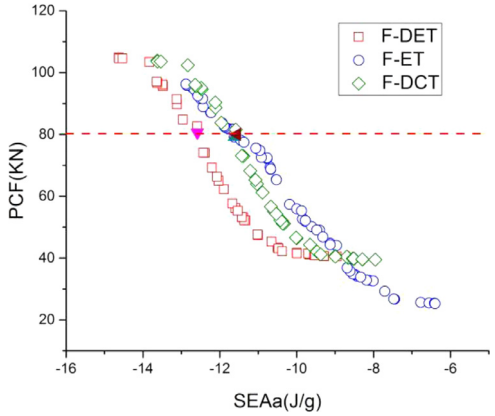

Fig. 14. Pareto fronts of the F-DET, F-ET and F-DCT tubes with load angle uncertainty.

PCF^0 for the optimal design of F-DET, F-ET, F-DCT tubes. Therefore the Kriging model is available to predict the crashworthiness performance. The radial rate f of optimal tubes are 0.564 and 0.648. It proves the superiority of the ellipse cross-section to some extend. In addition, the SEA_{α} of the F-DET tube is 11.77% higher than the F-ET tube and 10.51% higher than the F-DCT tube, which indicates F-DET tube is indeed a promising energy-absorbing configuration.

5. Conclusion

In this study, a novel foam-filled double ellipse tube is proposed. First, the circle and ellipse tubes with three different configurations(hollow, foam-filled, double foam-filled) are investigated under axial and oblique impact by using the nonlinear finite element code LS-DYNA. The numerical results showed that the foam-filled double ellipse tube has the best crashworthiness performance than tubes with other configurations. Thus, we focus on the optimization of the foam-filled double ellipse tube.

Then, based on the DOE results, the Kriging models of the foam-filled ellipse tube, the foam-filled double ellipse tube and foam-filled double circle tube are constructed. The optimal models of the F-DET, F-ET and F-DCT tubes are achieved by using the multiobjective particle swarm optimization (MOPSO) algorithm. After comparing the Pareto fronts of three kinds of tubes, it is obvious that the energy absorption capability per unit mass of the foam-filled double ellipse tubes is larger than the other two tubes. The SEA_{α} of the F-DET tube is 11.77% higher than the F-ET tube and 10.51% higher than the F-DCT tube at the condition that the PCF equals 80KN. This indicates that the F-DET tube is superior to the F-ET tube and F-DCT tube under the multiple loading.

Acknowledgements

This work was supported by Scientific Research and Industry Promotion Project of Jiangsu Provincial Education Department, China, under the grant number BY2014004-04, Scientific Research and Industry Promotion Project of Nanjing, under the grant number 201306011.

References

[1] Alghamdi AAA. Collapsible impact energy absorbers: an overview. Thin Wall Struct 2001;39:189–213.
[2] Aktay L, Kröplin BH, Toksoy AK, Güden M. Finite element and coupled finite element/smooth particle hydrodynamics modeling of the quasi-static crushing of empty and foam-filled single, bitubular and constraint hexagonal- and square–packed aluminum tubes. Mater Des 2008;29:952–62.
[3] Goel MD. Deformation, energy absorption and crushing behavior of single-, double- and multi-wall foam filled square and circular tubes. Thin Wall Struct 2015;90:1–11.
[4] Li Z, Yu J, Guo L. Deformation and energy absorption of aluminum foam-filled tubes subjected to oblique loading. Int J Mech Sci 2012;54:48–56.
[5] Qi C, Yang S. Crashworthiness and lightweight optimisation of thin-walled conical tubes subjected to an oblique impact. Int J Crashworthiness 2014;19:334–51.
[6] Santosa SP, Wierzbicki T, Hanssen AG, Langseth M. Experimental and numerical studies of foam-filled sections. Int J Impact Eng 2000;24:509–34.
[7] Toksoy AK, Güden M. Partial Al foam filling of commercial 1050H14 Al crash boxes: the effect of box column thickness and foam relative density on energy absorption. Thin Wall Struct 2010;48:482–94.
[8] Yin H, Wen G, Liu Z, Qing Q. Crashworthiness optimization design for foam–filled multi-cell thin-walled structures. Thin Wall Struct 2014;75:8–17.
[9] Ahmad Z, Thambiratnam DP, Tan ACC. Dynamic energy absorption characteristics of foam-filled conical tubes under oblique impact loading. Int J Impact Eng 2010;37:475–88.
[10] Aktay L, Toksoy AK, Güden M. Quasi-static axial crushing of extruded polystyrene foam-filled thin-walled aluminum tubes: experimental and numerical analysis. Mater Des 2006;27:556–65.
[11] Gao Q, Wang L, Wang Y, Wang C. Crushing analysis and multiobjective crashworthiness optimization of foam-filled ellipse tubes under oblique impact loading. Thin Wall Struct 2016;100:105–12.
[12] Toksoy AK, Güden M. The strengthening effect of polystyrene foam filling inaluminum thin-walled cylindrical tubes. Thin Wall Struct 2005;43:333–50.
[13] Gameiro CP, Cirne J. Dynamic axial crushing of short to long circular alu-minium tubes with agglomerate cork filler. Int J Mech Sci 2007;49:1029–37.
[14] Yin H, Wen G, Hou S, Chen K. Crushing analysis and multiobjective crash-worthiness optimization of honeycomb-filled single and bitubular polygonaltubes. Mater Des 2011;32:4449–60.
[15] Alavi Nia A, Parsapour M. An investigation on the energy absorption characteristics of multi-cell square tubes. Thin Wall Struct 2013;68:26–34.
[16] Hong W, Fan H, Xia Z, Jin F, Zhou Q, Fang D. Axial crushing behaviors of multi-cell tubes with triangular lattices. Int J Impact Eng 2014;63:106–17.
[17] Najafi A, Rais-Rohani M. Mechanics of axial plastic collapse in multi-cell, multi-corner crush tubes. Thin Wall Struct 2011;49:1–12.
[18] Tang Z, Liu S, Zhang Z. Analysis of energy absorption characteristics of cylindrical multi-cell columns. Thin Wall Struct 2013;62:75–84.
[19] Hanssen AG, Langseth M, Hopperstad OS. Static and dynamic crushing of circular aluminium extrusions with aluminium foam filler. Int J Impact Eng 2000;24(5):475–507.
[20] Hanssen AG, Langseth M, Hopperstad OS. Static and dynamic crushing of square aluminium extrusions with aluminium foam filler. Int J Impact Eng 2000;24(4):347–83.
[21] Han DC, Park SH. Collapse behavior of square thin-walled columns subjected to oblique loads. Thin-walled Struct 1999;35:167–84.
[22] Li ZB, Yu JL, Guo LW. Deformation and energy absorption of aluminum foam–filled tubes subjected to oblique loading. Int J Mech Sci 2012:48–56.
[23] Nagel G, Thambiratnam D. A numerical study on the impact response and energy absorption of tapered thin-walled tubes. Int J Mech Sci 2004;46:201–16.
[24] Nagel G, Thambiratnam D. Computer simulation and energy absorption of tapered thin-walled rectangular tubes. Thin-Wall Struct 2005;43:1225–42.
[25] Nagel G, Thambiratnam D. Dynamic simulation and energy absorption of tapered thin-walled tubes under oblique impact loading. Int J Impact Eng 2006;32:1595–620.
[26] Hou SJ, Li Q, Long S, Yang X, Li W. Crashworthiness design for foam filled thin-wall structures. Mater Des 2009;30(6):2024–32.
[27] Zhang Y, Sun GY, Li GY, Luo Z, Li Q. Optimization of foam-filled bitubal structures for crashworthiness criteria. Mater Des 2012;38:99–109.
[28] Guo LW, Yu JL. Bending behavior of aluminum foam-filled double cylindrical tubes. Acta Mech 2011;222:233–44.
[29] Haghi Kashani M, Shahsavari Alavijeh H, Akbarshahi H, Shakeri M. Bitubular square tubes with different arrangements under quasi-static axial compression loading. Mater Des 2013;51:1095–103.

[30] Ahmad Z, Thambiratnam DP. Crushing response of foam-filled conical tubes under quasi-static axial loading. Mater Des 2009;30:2393–403.
[31] Yin HF, Wen GL, Hou SJ, Qing QX. Multiobjective crashworthiness optimization of functionally lateral graded foam-filled tubes. Mater Des 2013;44:414–28.
[32] Reyes A, Hopperstad OS, Langseth M. Aluminum foam-filled extrusions subjected to oblique loading: experimental and numerical study. Int J Solids Struct 2004;41(5–6):1645–75.
[33] Wierzbicki T. Optimum design of integrated front panel against crash. Report for Ford Motor Company 1983:7–15.
[34] Li G, et al. Comparison of functionally-graded structures under multiple loading angles. Thin-Walled Struct 2015;94:334–47.
[35] Li ZB, Yu JL, Guo LW. Deformation and energy absorption of aluminum foam–filled tubes subjected to oblique loading. Int J Mech Sci 2012:48–56.
[36] Simpson Timothy W, Mauer M, Korte John J, Farrokh M. Kriging models for global approximation in simulation-based multidisciplinary design optimization. AIAA J 2001;39:2233–41.
[37] Raquel C, Naval P. An effective use of crowding distance in multiobjective particle swarm optimization. In: Proceedings of the 2005 conference on genetic and evolutionary computation; 2005. p. 257–64.